Use of Breeding to Detect and Explain Instabilities in the Global Ocean

M. J. Hoffman[1], E. Kalnay[2], J. A. Carton[2], and S. C. Yang[3]

[1]Department of Mathematics, University of Maryland, College Park, Maryland, USA.

[2]Department of Atmospheric and Oceanic Science, University of Maryland, College Park, Maryland, USA.

[3]Department of Atmospheric Science, National Central University, Jhongli, Taiwan.

Abstract

The breeding method of Toth and Kalnay, developed for atmospheric data assimilation studies, is applied to a global ocean model in order to identify instabilities as a function of timescale. In addition to exploring its usefulness in the oceanic context, this study extends the method to show how the energy equations for the bred vectors can be used to assess the characteristics of the instabilities. The approach is applied to diagnose instabilities occurring in the tropical Pacific and the South Atlantic.

1. Introduction

Previous examinations of the structure and causes of flow instabilities in the ocean have generally required consideration of time averages of the kinetic and potential energy equations (e.g., Pinardi and Robinson, 1986; Ducet et al., 2000) or even a full linear instability analysis (Huck and Vallis, 2001). However, the process of time averaging reduces the ability of this approach to discriminate among several concurrent instabilities with differing time-evolutions. Here we explore the potential of the breeding method to isolate and identify the aspects of time-dependent ocean flows that are unstable to small perturbations. The method was originally developed both for application to data assimilation (to identify the growing component of the analysis error (Yang et al., 2008)) and to provide a set of plausible initial conditions for ensemble forecasting of atmospheric motions representative of the growing errors in the analysis (Toth and Kalnay, 1993, 1997). Here we extend the method to provide an alternative view of the energetics of the global upper ocean which also has advantages of being simple to implement and computationally inexpensive.

The breeding method begins with an arbitrary small perturbation of the initial state of an unstable system, such as the atmosphere, represented by a numerical model. This model is integrated forward for a time interval, Δt, beginning from both the perturbed and unperturbed (or control) initial state. The vector difference in state variables (u, v, w, T, S) between the two resulting nonlinear forecasts is called the bred vector. At Δt this bred vector is rescaled to the size of the initial perturbation and then is added to the control simulation to form the perturbed initial state for a new simulation. Twin simulations beginning with the control and newly perturbed control initial state at Δt are then integrated forward from Δt to 2Δt to create a new simulation pair. The bred vector at time 2Δt is then computed, rescaled, and the process is repeated. When carried out over many cycles, the resulting time series of bred vectors has been shown by Toth and Kalnay to isolate and identify the components of the system that grow most rapidly on a time-scale of Δt, and to separate them from other rapidly growing components that saturate in times shorter than Δt. By varying Δt (hereafter known as the "breeding interval"), Peña and Kalnay (2004) showed how to isolate instabilities of different temporal scales. The bred vectors created by this process are essentially non-linear generalizations of Lyapunov vectors and, like these Lyapunov vectors, they are independent of the norm (such as root mean square size of the SST bred vector) chosen for rescaling (Toth and Kalnay, 1997; Kalnay et al., 2003). In fact, the shape of the bred vectors is dependent only on the size to which they are rescaled and the time interval between rescalings. It is through tuning these two parameters that the breeding method can be used to isolate different types of instabilities (Peña and Kalnay, 2004; Chikamoto et al., 2007; Vikhliaev et al., 2007).

Like the atmosphere, upper ocean currents are subject to a variety of flow instabilities. These instabilities are concentrated in regions of strong currents such as the western sides of subtropical gyres and the deep tropics where eddy kinetic energy may exceed 4500 cm s^{-2} (Ducet et al., 2000). However, the combination and dynamical balances within these instabilities, as well as their temporal and geographic variations, remains an active area of research. Many currents, such as the Agulhas, Kuroshio, Gulf Stream, Brazil, Malvinas, and Antarctic Circumpolar Currents, have a fairly constant level of eddy variability year round. Others, such as the North Equatorial Counter Current (NECC) of the tropical Pacific, show strong seasonality. For the NECC instability generated eddy kinetic energy reaches a maximum at 10°N in summer (Ducet et al., 2000). A little south of the NECC, in the latitude range

3°N-6°N, tropical instability waves (TIWs) occur in the longitude band between 180° and 120°W longitude. These TIWs also have a have a well defined seasonal cycle, with activity beginning in August and continuing through March of the next year (Masina et al., 1999).

Beginning with Philander (1976) there has been a long running discussion in the literature regarding the relative importance of baroclinic, barotropic, and frontal instabilities in providing the energy source for these TIWs. For example, Masina et al. (1999) suggest that there are two distinct locations of energy conversion with baroclinic conversion occurring between 3°N and 5°N and barotropic energy conversion occurring further equatorward. The strength of the TIWs is closely tied to the phase of ENSO, with the diminished strength of SST front in El Niño years leading to a decrease in TIW production and the increased SST front of La Niña causing stronger TIW activity (Contreras, 2002).

To explore the potential of the breeding approach in examining fluid instabilities in the ocean we extend the breeding method by defining the potential and kinetic energy equations for the perturbations and use these to explore instabilities in an ocean general circulation model driven by observed winds. In our discussion, we compare the results of this new approach with more traditional methods.

2. Model and Methods

The quasi-global ocean used in this study uses Geophysical Fluid Dynamics Laboratory (GFDL) Modular Ocean Model v.2 primitive equation numerical formulation with 1°x1° horizontal resolution in midlatitudes reducing to 1°x½° at the equator in order to resolve the intense equatorial current systems. The model domain extends 62.5°S-62.5°N, excluding the Arctic Ocean to prevent numerical difficulties associated with the convergence of the meridians. The model has 20 fixed depth levels in the vertical with 15m resolution near the surface expanding to 737m near the bottom. Horizontal and vertical mixing and heat and salt diffusion parameters are set as described in Carton et al. (2000) in order to reproduce the mean circulation. Initial conditions of climatological temperature and salinity are obtained from the World Ocean Atlas 1994 (Levitus and Boyer, 1994), while monthly winds are provided by the National Centers for Environmental Prediction (NCEP) reanalysis (Kalnay et al., 1996). Surface heat

and freshwater flux are calculated using a simple Haney-type relaxation to climatological monthly temperature and salinity.

To begin the breeding process, a random perturbation with values between -0.5°C and 0.5°C is introduced into the initial conditions for the sea surface temperature (SST) field. The remaining experiments reported here all use this same initial perturbation. Other experiments using different randomly chosen initial perturbations or perturbations in the velocity field yield similar results, confirming the earlier observation by Toth and Kalnay (1993, 1997) that the structure of the bred vectors is independent of the initial perturbation.

The derivation of the bred vector conservation of kinetic and potential energy equations (see *Auxiliary Material*) resembles that of the more common perturbation energy equations (Orlanski et al. 1991; Oczkowski et al. 2005) although, due to the fact that both the control and the perturbed nonlinear runs satisfy exactly the model equations, the bred vector equations are exact and do not require Reynolds averaging. Bred vector kinetic energy is defined as $KE_b \equiv (\vec{V}_b \cdot \vec{V}_b)/2$ where $\vec{V}_b$ is the bred vector horizontal velocity. Substituting this definition into the momentum equations, where $\vec{V}_c$ is the control run horizontal velocity, leads to:

$$\frac{\partial KE_b}{\partial t} = -\left[\nabla \cdot (\overrightarrow{V_c} KE_b) + \frac{\partial}{\partial z}(w_c KE_b)\right] - \left[\nabla \cdot (\overrightarrow{V_b} p_b) + \frac{\partial}{\partial z}(w_b p_b)\right] - w_b g \rho_b - \rho_0 \left[\overrightarrow{V_b} \cdot (\overrightarrow{V_b} \cdot \nabla)\overrightarrow{V_c} + \overrightarrow{V_b} \cdot \left(w_b \frac{\partial \overrightarrow{V_c}}{\partial z}\right)\right] + \overrightarrow{F_b} \quad (1)$$

where w_b and w_c are bred and control vertical velocities, p_b is bred vector pressure, and ρ_b is bred vector density ($\boldsymbol{\rho_{perturbation} = \rho_0 + \rho_c + \rho_b}$). The first bracketed term is horizontal and vertical divergence of the kinetic energy transport, and vanishes when integrated over the whole domain. The second is the work of the pressure force, the third is the baroclinic energy conversion from perturbation potential to perturbation kinetic energy, the fourth is barotropic energy conversion from background kinetic to bred kinetic energy, and the fifth term is a friction term. The friction term and vertical transports are generally negligible in the problems considered here.

Similarly, bred vector potential energy, defined as $\boldsymbol{PE_b \equiv \rho_b^2 g^2 / 2\rho_0}$, has the following equation:

$$\frac{\partial PE_b}{\partial t} = -\left[\nabla \cdot \left(\overrightarrow{V_c}\nabla PE_b\right) + \frac{\partial}{\partial z}\left(w_c PE_b\right)\right] + w_b g \rho_b - \frac{\rho_b g^2}{\rho_0 N^2}\left[\nabla \cdot \left(\overrightarrow{V_b}\rho_c\right) + \frac{\partial (w_b \rho_c)}{\partial z}\right] \qquad (2)$$

$$-w_c \frac{\partial PE_b}{\partial z}$$

The first bracketed term is horizontal and vertical divergence of the potential energy transport, and vanishes when integrated over the whole domain. The second term is baroclinic energy conversion and has the opposite sign of the corresponding term in the kinetic energy equation. The third term is negligible, since it is proportional to the perturbations in density times a term that vanishes when integrated over the whole domain. The last term is also negligible. In this Letter we focus mainly on interpreting the bred vector kinetic energy equation.

Results from control and bred vector simulations spanning two periods are examined, a multi-decadal period beginning January 1951 through December 1979 and a shorter, observation-rich period spanning the eight year period January 1985 through December 1992. Due to space limitations we will focus on the latter period, although the longer run is used to compute climatological monthly averages. A monthly breeding interval is used for the shorter simulation, while a 10 day breeding interval is used for the longer simulation to better isolate the period of TIWs.

3. Results

We begin by considering the bred vector energy balance on 11 November 1988, a time when the tropical Pacific was in a late developing La Niña (with a Southern Oscillation Index of 21.0 and a Nino3.4 Index value of -2^{o}C). The bred vector shows a dipole pattern off the coast of South America and a wave pattern further west (**fig. 1a**) which successive bred vectors show to have a period of ~25 days and to propagate westward at 0.46m/s. Examination of the bred vector energetics shows that baroclinic processes are causing an increase in bred vector kinetic energy along the equator (**fig. 1b)**. In the region of the dipole pattern off the coast of South America, by contrast, there is a conversion from bred vector kinetic to potential energy consistent with a transfer of bred vector kinetic energy from the atmosphere to the ocean, which is then converted into bred vector potential energy.

We next consider the interannual dependence of the energy conversion terms (**fig 2**). Both baroclinic and barotropic energy conversion terms spike during August through January, with the size of the spike varying by year. The strongest spikes of energy conversion occur in the La Niña years of 1984-1985 and 1988-1989 when the TIWs, NECC, and Equatorial Undercurrent are all anomalously strong. Bred vector baroclinic energy conversion is maximum between 3°N and 5°N, with conversion increasing in August between 150°W and 130°W and shifting westward past 170°W by the end of the year (**fig. 2**). In contrast, bred vector energy conversion is weak during the 1991-1992 El Niño when the Equatorial Undercurrent has reduced transport and TIWs are weak.

Finally, we examine the geographic and vertical structure of the seasonal cycle of bred vector energy conversion. The majority of the baroclinic conversion occurs above the thermocline, with the strongest conversion taking place in the upper 100 meters (**fig. 3a**). The longitude of this maximum baroclinic conversion corresponds to the location of the tongue of cool SSTs and consequent strong meridional SST gradient. Barotropic conversion also occurs in this region and along the equator between 160°W and 140°W (**fig. 3b**) although it takes place deeper than baroclinic conversion, with the strongest conversion at and just below the shear zone between the westward South Equatorial Current and the eastward Equatorial Undercurrent. Bred vector barotropic conversion can also be seen in the same 3°N to 5°N latitude band, just south of the NECC, as baroclinic conversion.

4. Summary

The purpose of this Letter is to apply bred vectors, an idea developed in the context of atmospheric data assimilation, to stability analysis of ocean circulation. As part of this application we introduce the bred vector energy equations, which are analogous to the more traditional eddy energy equations but are obtained *without approximations* or averaging due to the fact that both the control and the perturbed runs satisfy the model dynamical equations. We find, consistent with findings reported in Yang et al. (2006), that changes in bred vector energy reflect important aspects of the growth of flow instabilities. Thus, breeding, the process by which the bred vectors are constructed, is able to identify ocean instabilities effectively and inexpensively. Because they span the state space described by key ocean processes, bred vectors also have potential applications in the construction of ensembles of model states for ensemble data assimilation and forecasting.

Our examination of bred vectors in the global ocean focuses on instabilities of tropical Pacific currents because of their intensity, their importance for coupled air-sea interactions, and because of the extensive literature describing them. Examination of the bred vector energy equations shows that there are two locations of energy conversion for the tropical instability waves which dominate intraseasonal variability in this region. Between 3°N and 5°N, both baroclinic and barotropic energy conversion occurs along the northern edge of the cool tongue. A separate region of barotropic conversion is detected just north of the equator in the shear zone between the Equatorial Undercurrent and the shallower South Equatorial Current, e.g. in agreement with Massina et al. (1999). Both types of energy conversion have interannual variations due to changes in the currents and stratification, which are themselves closely tied to the phase of ENSO.

Acknowledgements

This work was supported in part by the National Science Foundation grant OCE0752209 to JAC, and NASA grant NNG06B77G to EK. We would like to thank Drs. Gennady Chepurin, Chris Danforth, Semyon Grodsky, and Raghu Murtugudde for their helpful comments and suggestions. This work forms a part of the dissertation research of MJH.

References

Carton, J.A., G.A. Chepurin, X. Cao, and B.S. Giese (2000a), A Simple Ocean Data Assimilation Analysis of the Global Upper Ocean 1950-1995, Part 1: Methodology, *J. Phys. Oceanogr.*, *30*, 294-309.

Carton, J.A., G.A. Chepurin, and X. Cao (2000b), A Simple Ocean Data Assimilation Analysis of the Global Upper Ocean 1950-1995 Part 2: Results, *J. Phys. Oceanogr.*, *30*, 311-326.

Chikamoto, Y., H. Mukougawa, T. Kubota, H. Sato, A. Ito, and S. Maeda (2007), Evidence of growing bred vector associated with the tropical interseasonal oscillation, *Geophys. Res. Let.*, *34*, L04806, doi:10.1029/2006GL028450.

Contreras, R. F. (2002), Long Term Observations of Tropical Instability Waves, *J. Phys. Oceanogr.*, *32*, 2715-2722.

Ducet N., P.Y. Le Traon, and G. Reverdin (2000), Global high-resolution mapping of ocean circulation from TOPEX/Poseidon and ERS-1 and-2. *J. Geophys. Res.-Oceans*, *105*, 19477-19498.

Halpern, D., R. A. Knox, and D. S. Luther (1988), Observations of 20-Day Period Meridional Current Oscillations in the Upper Ocean along the Pacific Equator, *J. Phys. Oceanogr.*, *18*, 1514-1534.

Huck, T., and G.K. Vallis (2001), Linear stability analysis of the three-dimensional thermally-driven ocean circulation : application to interdecadal oscillations, *Tellus Series A*, *53*, 526-545.

Kalnay, E. (2004), *Atmospheric Modelling, Data Assimilation and Predictability*, Cambridge University Press, Cambridge, UK.

Kalnay, E., et at. (1996), The NCEP/NCAR 40-year reanalysis project, *Bull. Am. Meteorol. Soc.*, *77*, 437-471.

Legeckis, R. (1977), Long waves in eastern equatorial Pacific Ocean-View from a geostationary satellite, *Science*, *197*, 1179-1181.

Levitus, S and T. Boyer (1994), *World Ocean Atlas 1994, Vol. 4: Temperature*, NESDIS Atlas series, NOAA, Washington, DC.

Masina, S. and S. G. H. Philander (1999), An analysis of tropical instability waves in a numerical model of the Pacific Ocean 1. Spatial variability of the waves, *J. Geophys. Res.*, *104*, 29613-29635.

Masina, S., S. G. H. Philander, and A. B. G. Bush (1999), An analysis of tropical instability waves in a numerical model of the Pacific Ocean 2. Generation and energetics of the waves, *J. Geophys. Res.*, *104*, 29637-29661.

Orlanski, I., and J. J. Katzfey (1991), The life cycle of a cyclone wave in the Southern Hemisphere. Part I: Eddy energy budget, *J. Atmos. Sci.*, *48*, 1972-1998.

Oczkowski, M., I. Szunyogh, and D.J. Patil (2005), Mechanisms for the Development of Locally Low Dimensional Atmospheric Dynamics, *J. Atmos. Sci.*, *62*, 1135-1156.

Peña, M. and E. Kalnay (2004), Separating fast and slow modes in coupled chaotic systems, *Nonlinear Process. Geophys.*, *11*, 319-327.

Philander, S. (1976), Instabilities of zonal equatorial currents-Part 1. *J. Geophys. Res*., *81*, 3725-3735.

Pinardi, N. and A. R. Robinson (1986), Quasigeostrophic energetics of open ocean regions, *Dynamics of Atmosphere and Oceans*, *Vol. 10*(3), 185-221.

Qiao, L. and R. H. Weisberg (1998), Tropical Instability Wave Energetics: Observations from the Tropical Instability Wave Experiment, *J. Phys. Oceanogr.*, *28*, 345-360.

Toth, Z., and E. Kalnay (1993), Ensemble Forecasting at NMC: The Generation of Perturbations, *Bull. Amer. Meteorol. Soc.*, *74*, 2317-2330.

Toth, Z., and E. Kalnay (1997), Ensemble Forecasting at NCEP and the Breeding Method, *Mon, Wea. Rev.*, *125*, 3297-3319.

Vikhliaev, Y., B. Kirtman, and P. Schopf (2007), Decadal North Pacific Bred Vectors in a Coupled GCM, *J. Clim*., *20*, 5744–5764.

Yang, S.-C., M. Cai, E. Kalnay, M. Rienecker, G. Yuan, and Z. Toth (2006), ENSO bred vectors in coupled ocean-atmosphere general circulation models, *J. Clim.*, *19*, 1422-1436.

Yang S.-C., C. Keppenne, E. Kalnay (2008), Applications of coupled bred vectors to seasonal-to-interannual forecasting and ocean data assimilaiton, Submitted to *J. Clim*.

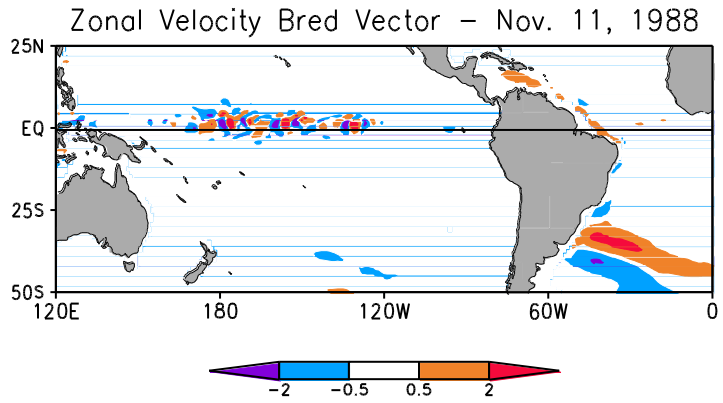

(a)

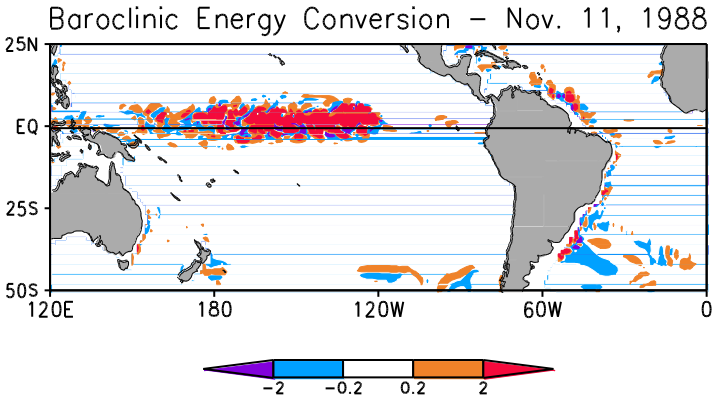

(b)

Figure 1 (a) Bred vector of zonal velocity on 11 November 1988, a time when the tropical Pacific was in a late developing La Niña with a Southern Oscillation Index of 21.0 and a Nino3.4 Index of -2°C. (b) Corresponding baroclinic energy conversion term (see Eqn. 1). Baroclinic energy conversion contributes to the growth of bred vector kinetic energy along the Pacific equator. Off the coast of South America the baroclinic conversion term acts to convert bred vector kinetic to potential energy. The magnitudes of the fields are somewhat arbitrary due to the rescaling of the bred vectors, but the units are m/s for the velocity and 10^{-6} Watts for the baroclinic energy conversion.

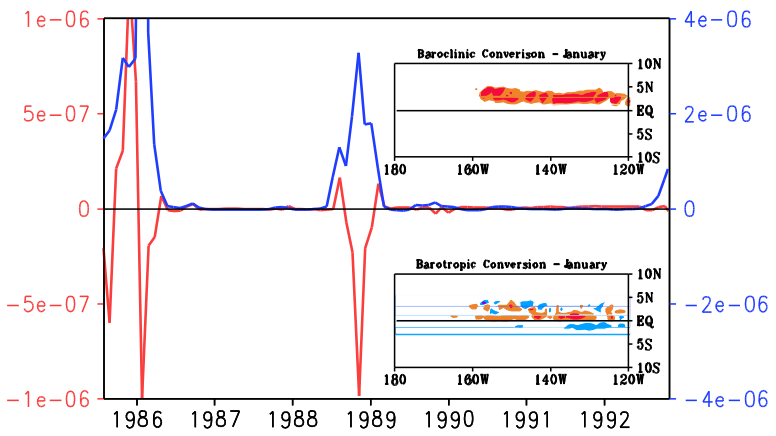

Figure 2: The red and blue lines show the time series from 1985 to 1992 of conversion terms averaged in a box 180°W to 120°W, -5°S to 5°N latitude, and between the surface and 150m depth. The barotropic conversion term is shown in red while the baroclinic conversion term is shown in blue. The inlayed panels show the 30 year averages of the baroclinic and barotropic conversion terms for the month of January, during which barotropic energy has a peak and baroclinic energy is very strong. For the barotropic conversion term (bottom inlaid panel) two distinct regions of energy conversion are visible: one between 3°N and 5°N, which mirrors the baroclinic conversion term (top panel), and the other just above the equator. It is important to note that the sign and relative magnitude of the bred vector energy conversion terms indicate the shape, direction, and location of the energy conversion. However, because the bred vectors are rescaled to a predetermined value, the absolute magnitude of the energy conversion should not be considered accurate.

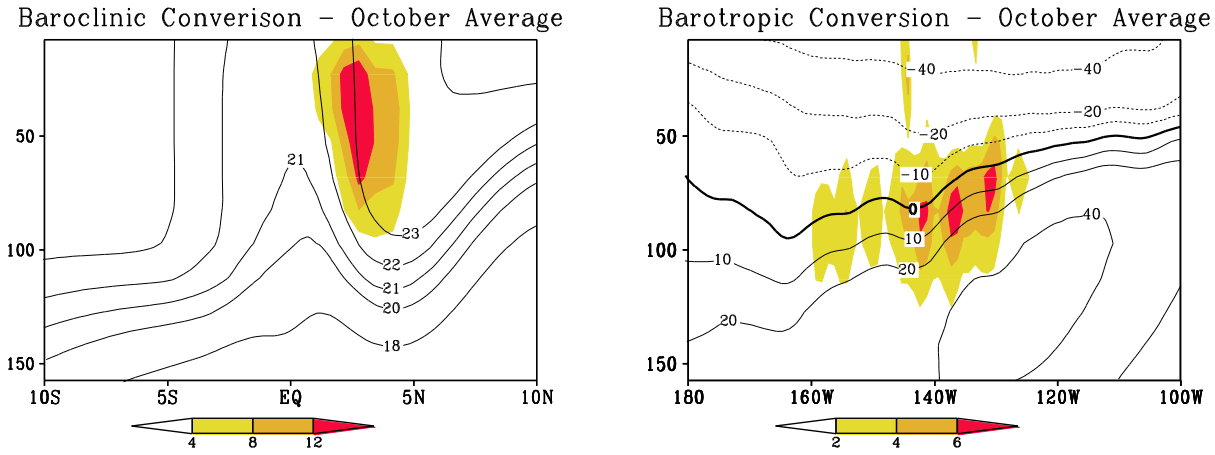

Figure 3: Vertical profile of climatological October properties computed from the 30 year monthly average. (a) Baroclinic conversion term (shaded) and temperature (contours) with latitude between 180° to 110°W, and (b) barotropic conversion term (shaded) and zonal velocity (contours) with longitude at 0.65°N. Baroclinic conversion from potential to kinetic bred perturbation energy occurs above the thermocline with maximum at the latitude of coldest SST. The maximum barotropic conversion from the background kinetic energy to the bred perturbation occurs along the shear zone between the westward South Equatorial Current and eastward Equatorial Undercurrent.